*The following supplements accompany the article*

# Habitat- and sex-specific life history patterns of yellow tang *Zebrasoma flavescens* in Hawaii, USA

**Jeremy T. Claisse[1,*], Marco Kienzle[2], Megan E. Bushnell[1], David J. Shafer[1], James D. Parrish[1]**

**[1]University of Hawaii, Department of Zoology, 2538 McCarthy Mall, Edmondson 165, Honolulu, Hawaii 96822, USA**
**[2]CSIRO, Marine and Atmospheric Research Division, 233 Middle Street, Cleveland, Queensland 4163, Australia**

**Email: claisse@hawaii.edu*

*Marine Ecology Progress Series 389:245–255 (2009)*

**Supplement 1.** Validation of annual periodicity of increment formations.

## MATERIALS AND METHODS

To validate the annual nature of increment formation in the sagittae of juveniles and adults, an additional 146 yellow tang (58 to 183 mm total length [TL]) were captured along the west coast of Hawaii Island, Hawaii, injected with a dosage of 50 mg $kg^{-1}$ body weight of tetracycline HCL in a sterile saline solution into their musculature (McFarlane & Beamish 1987) and then released at their capture site. All tetracycline-tagged fish also received unique visible external marks. Thirty-six of these marked fish were recaptured 14 to 15 mo later. Otoliths were removed and sectioned as described in 'Materials and methods' in the main article. Care was taken not to expose the otoliths to light for extended periods to avoid compromising the intensity of the tetracycline fluorescent marker. To visualize the tetracycline band within the otoliths, they were viewed with an Olympus BX-51 fluorescence microscope outfitted with a U-MWB2 filter cube (EX460-490, DM500, EM520IF) and photographed with a digital camera. The periodicity of opaque zone formation was estimated following Cappo et al. (2000). Otolith weight was regressed on age, as a strong, positive relationship would indicate continuous otolith growth throughout the lifespan (Fowler & Doherty 1992, Choat & Axe 1996).

## RESULTS

The 36 recaptured yellow tang previously injected with tetracycline ranged in size from 85 to 182 mm TL. All specimens displayed an identifiable tetracycline mark under the flourescence microscope which appeared yellow compared to the green color of the rest of the otolith structure. In 33 of the 36 total otoliths, the distance from the tetracycline band to other structural elements could be measured to permit estimation of the periodicity of increment formation (Cappo et al. 2000). Periodicity was estimated to be 0.98 increments $yr^{-1}$, supporting an annual pattern of increment formation. The 3 remaining otoliths displayed a single opaque zone outside the parts of the tetracycline mark that were visible, consistent with annual increment formation. Otoliths in the present study were consistent with all 3 criteria for use in age-based approaches described in Fowler & Doherty (1992): (1) they displayed an internal structure of increments that were (2) related to a regular time scale of formation, and (3) a significant ($p < 0.001$) positive relationship was found between otolith weight and age [log(weight) = −2.67 + 0.542 log(age); $R^2$ = 88.9%], indicating otolith growth throughout the lifespan.

## **Supplement 2.** Model selection

Biological hypotheses were investigated via model selection (Burnham & Anderson 2002) using the second-order bias corrected Akaike's Information Criterion (AICc). AICc includes an additional term to correct for bias related to small sample size (n) that becomes negligible when n is large (Akaike 1973, Anderson 2008). Akaike weights ($w_i$) were calculated to assess the relative likelihood of each model in a set and were interpreted as a weight of evidence in favor of the hypothesis represented by the model (Burnham & Anderson 2002).

The hypothesis of sexual differences in median size and age at ontogenetic habitat shift was examined using parameterizations of the logistic habitat use model fitted to either length (Table S2.1) or age (Table S2.2) from the habitat-specific collections. Each model set contains one model with identical parameters for both sexes, assuming no sexual difference in habitat use patterns and one model with separate parameters for each sex, allowing for unique median lengths or ages for males and females.

Sexually dimorphic differences in growth at age were examined with a set of models containing various parameterizations of both the von Bertalanffy growth function (VBGF) and the reparameterized VBGF (rVBGF), each representing a specific hypothesis. Absence of sexual growth dimorphism was modeled using VBGF (and rVBGF) with identical parameters for both sexes (Table S2.3, Model 5). By contrast, sexual growth dimorphism can result from many different parameterizations of VBGF and rVBGF. Four models (Table S2.3, Models 1–4) were used to describe particular differences in growth trajectories between male and female. Model 1 allows for completely unique growth curves for each sex; Models 2 & 4 represent growth curves with equal length at age 2, but different length at age 7 and 12 or only at age 12, respectively; and Model 3 assumes that each sex has a different mean maximum length, while the time required to reach that size ($k^{-1}$) and the constant $t_0$ are equal for both sexes. Growth variability ($\sigma$) was estimated separately for each sex in all models that assumed sexual growth dimorphism.

The hypothesis of sexually dimorphic growth at length from capture-mark-recapture data was examined with a model set containing various parameterizations of the GROTAG model (Table S2.4). Absence of growth at length dimorphism was modeled using 2 parameterizations of the GROTAG model with identical parameters for both sexes (Table S2.4, Models 2 & 4). Conversely, 2 other parameterizations of the GROTAG model allowed for unique growth rate at length for males and females by including separate

Table S2.1. *Zebrasoma flavescens*. Model selection results for median length at ontogenetic habitat shift. Model parameters are either common for both sexes assuming no sexual differences in length at habitat shift or are unique sex-specific parameters. Models were ranked according to the difference in AICc (ΔAICc) and Akaike weight ($w_i$). $N_p$: number of estimated parameters in each model

| Model no. | Common parameters | Sex-specific parameters | ΔAICc | $w_i$ | AICc | $N_p$ |
|---|---|---|---|---|---|---|
| 1 | – | $\beta_0$, $\beta_1$ | 0.0 | 1.0 | 125.1 | 4 |
| 2 | $\beta_0$, $\beta_1$ | – | 108.9 | 0.0 | 234.0 | 2 |

Table S2.2. *Zebrasoma flavescens*. Model selection results for median age at ontogenetic habitat shift. Model parameters are either common for both sexes assuming no sexual differences in age at habitat shift or are unique sex-specific parameters. Models were ranked according to the difference in AICc (ΔAICc) and Akaike weight ($w_i$). $N_p$: number of estimated parameters in each model

| Model no. | Common parameters | Sex-specific parameters | ΔAICc | $w_i$ | AICc | $N_p$ |
|---|---|---|---|---|---|---|
| 1 | – | $\beta_0$, $\beta_1$ | 0.0 | 1.0 | 304.9 | 4 |
| 2 | $\beta_0$, $\beta_1$ | – | 28.6 | 0.0 | 333.5 | 2 |

Table S2.3. *Zebrasoma flavescens*. Von Bertalanffy growth function (VBGF) and reparameterized VBGF (rVBGF) model selection results. Model parameters either assume sexual dimorphism and are sex-specific or assume no sexual dimorphism and are common for the 2 sexes. Models were ranked according to the difference in AICc (ΔAICc) and Akaike weight ($w_i$). $N_p$: number of estimated parameters in each model

| Model no. | Common parameters | Sex-specific parameters | ΔAICc | AICc | $w_i$ | $N_p$ |
|---|---|---|---|---|---|---|
| 1 | – | $l_y$, $l_w$, $l_v$, $\sigma$ or $l_\infty$, $k$, $t_0$, $\sigma$ | 0.0 | 4700.4 | 0.95 | 8 |
| 2 | $l_y$ | $_w$, $l_v$, $\sigma$ | 4.6 | 4705.0 | 0.05 | 7 |
| 3 | $k$, $t_0$ | $l_\infty$, $\sigma$ | 18.4 | 4718.8 | 0 | 6 |
| 4 | $l_y$, $l_w$, | $l_v$, $\sigma$ | 183.9 | 4884.3 | 0 | 6 |
| 5 | $l_y$, $l_w$, $l_v$, $\sigma$ or $l_\infty$, $k$, $t_0$, $\sigma$ | – | 375.7 | 5076.1 | 0 | 4 |

parameters for each sex (Table S2.4, Models 1 & 3). The assumption of proportional increase in growth variability was also examined by including parameterizations of the GROTAG model in the model set where $v$ is held at 0 and any individual growth variability is thus included in $s$ (Table S2.4, Models 3 & 4) (Francis 1988).

Table S2.4. *Zebrasoma flavescens*. GROTAG model selection results. Parameterizations either assume dimorphism and contain separate sex-specific parameters, or assume no sexual dimorphism in growth and are common to the 2 sexes. Models were ranked according to the difference in AICc (ΔAICc) and Akaike weight ($w_i$). $N_p$: number of estimated parameters in each model

| Model no. | Common parameters | Sex-specific parameters | ΔAICc | $w_i$ | AICc | $N_p$ |
|---|---|---|---|---|---|---|
| 1 | – | $g_\alpha$, $g_\beta$, $v$, $s$ | 0 | 1.000 | 870.7 | 8 |
| 2 | $g_\alpha$, $g_\beta$, $v$, $s$ | – | 32.4 | 0.000 | 903.1 | 4 |
| 3 | – | $g_\alpha$, $g_\beta$, $s$ | 50.3 | 0.000 | 921.0 | 6 |
| 4 | $g_\alpha$, $g_\beta$, $s$ | – | 69.1 | 0.000 | 939.8 | 3 |

**Supplement 3.** Length–weight sexual dimorphic relationship

## METHODS

The assumed relationship between length and weight was modeled as:

$$W = aL^b \quad (1)$$

where $W$ is weight (g), $L$ is TL (mm) and $a$ and $b$ are 2 fitting parameters which have no direct biological meaning. This function was fitted by maximum likelihood, assuming that: (1) $W$ is normally distributed with mean given by Eq. (1); and (2) standard deviation (σ) increases as a square function of length × a constant $c$:

$$\sigma = cL^2 \quad (2)$$

Because we reasoned that the measurement error varies according to the derivative of the function and parameter b is often close to 3, the standard deviation should follow a function close to that shown in Eq. (2) (Taylor 1997). Examination of model residuals confirmed that these assumptions were appropriate.

The hypothesis of sexual dimorphism (estimating 3 parameters for each sex) was compared to the hypothesis of no sexual dimorphism (3 parameters estimated) via model selection using AICc (Akaike 1973, Anderson 2008).

Visual examination of the plotted data (Fig. S3.1) suggested possible dimorphism that could be due to increased ovary weight after sexual maturity was reached in females (>14 cm TL; Bushnell 2007). To investigate whether possible dimorphism resulted from large ovaries, we also fitted both models following the same procedure as above to the somatic weight (total weight – gonad weight) for all individuals for which gonad weight was available.

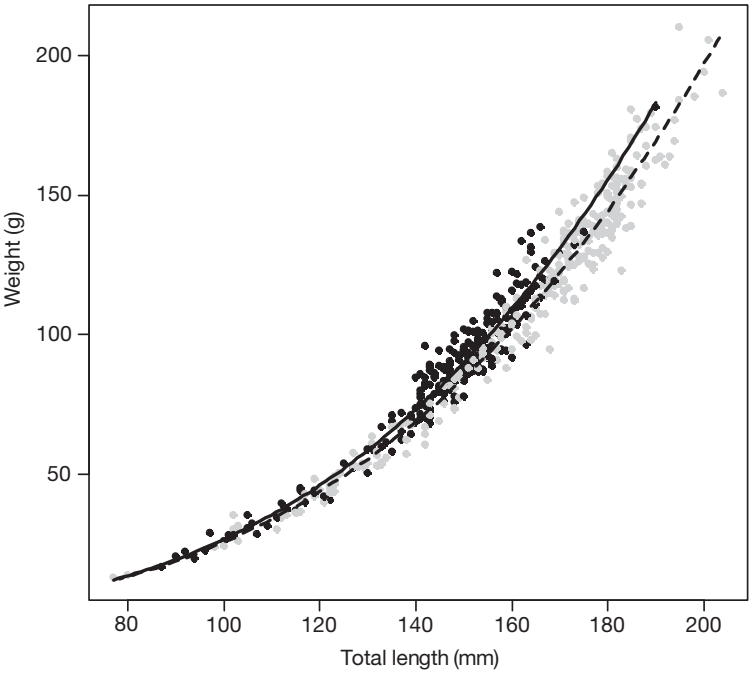


Fig. S3.1. *Zebrasoma flavescens.* Total length vs. weight relationship by sex: $W = aL^b$. Males: $a$ = 3.29E–05; $b$ = 2.94. Females: $a$ = 2.58E–05; $b$ = 3.01. Black circles and solid line are female, and grey circles and dashed line are male

## RESULTS AND DISCUSSION

Results of model selection and model parameter estimates are listed in Table S3.1. When total weight was used, model selection heavily favored the sexually dimorphic model and weight-at-length differences between the sexes were relatively small (Fig. S3.1) The difference in mean female total weight-at-length increased from around 3% higher than male weight at 80 mm TL to around 7% higher at 160 mm TL. When somatic weight was used, which removed the potential

Table S3.1. *Zebrasoma flavescens.* Sexually dimorphic length–weight relationship model selection results and parameter estimates. Analysis performed with total weight and again with somatic (total – gonad) weight. Models for each analysis ranked according to the difference in AICc (ΔAICc). $w_i$: Akaike weight; $N_p$: number of estimated parameters in each model; n: sample size; $c$: see 'Methods', this supplement

| Model | ΔAICc | AICc | $w_i$ | $N_p$ | n | Parameter estimates | | |
|---|---|---|---|---|---|---|---|---|
| | | | | | | $a$ | $b$ | $c$ |
| **Total weight** | | | | | | | | |
| Sexual dimorphism | 0 | 3590 | 1.000 | 6 | | | | |
| Male | | | | | 297 | 3.29E–05 | 2.94 | 2.67E–04 |
| Female | | | | | 248 | 2.58E–05 | 3.01 | 2.81E–04 |
| No dimorphism | 61 | 3674 | 0.000 | 3 | 545 | 5.16E–05 | 2.86 | 2.97E–04 |
| **Somatic weight** | | | | | | | | |
| Sexual dimorphism | 0 | 2851 | 1.000 | 6 | | | | |
| Male | | | | | 241 | 3.53E–05 | 2.93 | 2.53E–04 |
| Female | | | | | 196 | 2.89E–05 | 2.98 | 2.53E–04 |
| No dimorphism | 17 | 2868 | 0.000 | 3 | 437 | 4.96E–05 | 2.87 | 2.60E–04 |

influence that large ovary weight played in this relationship, the sexually dimorphic model continued to be strongly supported by our data. However, the sexual difference in weight-at-length decreased by about half, from <1 % at 80 mm TL increasing to around 4 % at 160 mm TL (Fig. A3.2). For most practical applications of a length–weight model, this difference may be negligible. Ovary weight can vary substantially both throughout the year and the lunar cycle (Bushnell 2007). Therefore, the presence of a sexually dimorphic length–weight relationship may depend considerably on time of sampling.

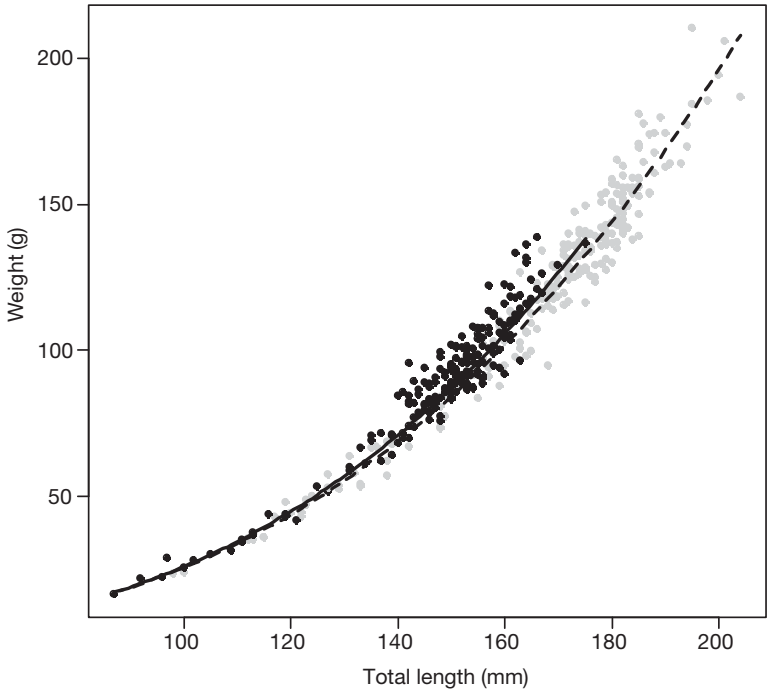


Fig. A3.2. *Zebrasoma flavescens.* Total length vs. somatic weight relationship by sex: $W = aL^b$. Males: $a$ = 3.53E−05; $b$ = 2.93. Females: $a$ = 2.89E−05; $b$ = 2.98. Black circles and solid line are female and grey circles and dashed line are male

LITERATURE CITED

Akaike H (1973) Information theory and an extension of the maximum likelihood principle. In: Petran BN, Csaki F (eds) Proc 2nd Int Symp Information Theory, Akademiai Kiadi, Budapest, p 267–281

Anderson DR (2008) Model based inferences in the life sciences: a primer on evidence. Springer Science, New York

Burnham KP, Anderson DR (2002) Model selection and multimodel inference, a practical information-theoretic approach. Springer Science, New York

Bushnell ME (2007) Reproduction of *Zebrasoma flavescens*: oocyte maturation, spawning patterns and an estimate of reproductive potential for female yellow tang in Hawaii. MS thesis, University of Hawaii, Manoa

Cappo M, Eden P, Newman SJ, Robertson S (2000) A new approach to validation of periodicity and timing of opaque zone formation in the otoliths of eleven species of *Lutjanus* from the central Great Barrier Reef. Fish Bull 98: 474–488

Choat JH, Axe LM (1996) Growth and longevity in acanthurid fishes; an analysis of otolith increments. Mar Ecol Prog Ser 134:15–26

Fowler AJ, Doherty PJ (1992) Validation of annual growth increments in the otoliths of two species of damselfish from the southern Great Barrier Reef. Mar Freshw Res 43: 1057–1068

Francis RICC (1988) Maximum likelihood estimation of growth and growth variability from tagging data. NZ J Mar Freshw Res 22:42–51

McFarlane GA, Beamish RJ (1987) Selection of dosages of oxytetracycline for age validation studies. Can J Fish Aquat Sci 44:905–909

Taylor JR (1997) An introduction to error analysis: the study of uncertainties in physical measurements, 2nd edn. University Science Books, Mill Valley, CA